Integrated control for pHRI:
Collision avoidance, detection, reaction and collaboration

Alessandro De Luca   Fabrizio Flacco

Abstract— We present an integrated control framework for safe physical Human-Robot Interaction (pHRI) based on a hierarchy of consistent behaviors. Safe human robot coexistence is achieved with a layered approach for coping with undesired collisions and intended contacts. A collision avoidance algorithm based on depth information of the HRI scene is used in the first place. Since collision avoidance cannot be guaranteed, it is supported by a physical collision detection/reaction method based on a residual signal which needs only joint position measures. On top of this layer, safe human-robot collaboration tasks can be realized. Collaboration phases are activated and ended by human gestures or voice commands. Intentional physical interaction is enabled and exchanged forces are estimated by integrating the residual with an estimation of the contact point obtained from depth sensing. During the collaboration, only the human parts that are designated as collaborative are allowed to touch the robot while, consistently to the lower layers, all other contacts are considered undesired collisions. Preliminary experimental results with a KUKA LWR-IV and a Kinect sensor are presented.

I. INTRODUCTION

Robotics research is quickly moving its focus from 'robots that can work in place of humans' to 'robots that can collaborate with humans'. This trend has been supported by emergent needs both in service and industrial robotics, e.g., elderly people needing physical help for their mobility or blue-collars requiring a reliable and accurate co-worker, and by the recent progresses in robotic hardware and software technology that allow a safer physical Human-Robot Interaction (pHRI).
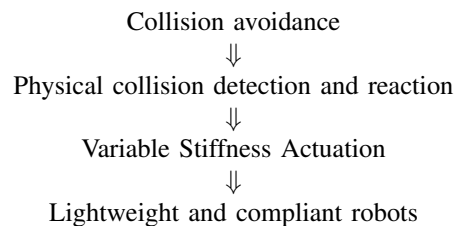
Safe pHRI can be conceived as nested layers of consistent behaviors that the robot must guarantee and accomplish:

$$\left\{ \left\{ \begin{array}{c} \{\text{Safety}\} \\ \text{Coexistence} \\ \text{Collaboration} \end{array} \right\} \right\}$$

Safety is the inherent and most important feature of a robot that has to work close to human beings. The classical solutions for preserving safety in industrial environments, i.e., using cages or stopping the robot in the presence of humans, are clearly inappropriate for pHRI. The latest industrial safety standards [1] and the technical specification ISO/TS15066 in preparation limit the total instantaneous power of a robotic system in operation and determine a maximum speed of moving robots in human environments. However, they may still fall short in some desired professional or personal service applications and research in this area may contribute in better understanding safety in human-robot coexistence.

The current approach for reducing the possibility of injuries to the humans [2], as well as of damages to the robot, merges several internal and external safety-oriented features, at the mechanical, sensory, and control levels, in an integrated top-down hierarchy. One possible scheme is:

Collision avoidance
$\Downarrow$
Physical collision detection and reaction
$\Downarrow$
Variable Stiffness Actuation
$\Downarrow$
Lightweight and compliant robots

The safest possible solution is namely to avoid any undesired contact (collision) with humans or environment obstacles [3], [4]. Unfortunately, collision avoidance may fail due to the limits of sensors and robot motion capabilities, e.g., if the human moves faster than the robot can sense or counteract. In this event, it is still possible to detect a physical collision and react to it [5]–[7], so as to immediately remove the robot from the collision area. Under such conditions, robots using Variable Stiffness Actuation (see, e.g., [8]–[10]), when properly controlled [11], [12], and lightweight robots with compliant joints [13] can be used to reduce the collision forces at the impact.

Coexistence is the robot capability of sharing the workspace with other entities, most relevant with humans in which case human safety requirements must be consistently guaranteed (i.e., safe coexistence). An example of coexistence (sometimes called also as coaction) is when a robot and a human operator work together on the same object, without ever requiring mutual contact or coordination of actions and intentions.

Collaboration is the robot feature of performing a complex task with direct human interaction and coordination in two different, not mutually exclusive modalities. In *physical* collaboration, there is an explicit and intentional contact with exchange of forces between human and robot. By measuring or estimating these forces, the robot can predict human motion intentions and react accordingly [14], [15]. In *contactless* collaboration, there is no physical interaction: coordinated actions are guided or follow from an exchange of information, which can be achieved via direct communication, like with gestures and/or voice commands [16], or indirect communication, by recognizing intentions [17] or attention [18], e.g., through eye gaze. We refer to safe

The authors are with the Dipartimento di Ingegneria Informatica, Automatica e Gestionale (DIAG, former DIS), Università di Roma "La Sapienza", Via Ariosto 25, 00185 Rome, Italy. Email: {deluca,fflacco}@dis.uniroma1.it

physical collaboration when this activity is consistent with safe coexistence, i.e., when safety and coexistence features are guaranteed during physical collaboration phases. For example, if the human is collaborating with the robot using his/her right hand, contact between the robot and the human head is undesired, and therefore such accidental collisions must be avoided. Similarly, if during a contactless collaboration the human enters the robot workspace, the human-robot system should be controlled so as to preserve safe coexistence.

In this paper, we present an integrated approach to safe-oriented robot control of pHRI. We elaborate on some of our previous results on physical collision detection (Sect. III) and robot reaction (Sect. IV), both using a residual-based method with only proprioceptive information, and on a collision avoidance method (Sect. V) that uses depth information as given by an exteroceptive sensor. The presented methods can be suitably modified and merged to allow a safe physical collaboration (Sect. VI), in particular for evaluating intentional contact forces between human and robot in the absence of contact/force sensing, as a necessary prerequisite for their control. The associated control algorithms have been implemented on a KUKA LWR-IV manipulator and tested on a scenario, equipped with a Kinect sensor, in which the robot performs a task in the presence of a human (Sect. VII). In safe coexistence conditions, the human operator activates and disactivates safe physical collaboration phases using gestures.

II. PRELIMINARIES

We consider robot manipulators as open kinematic chains of rigid bodies, having n (rotational) joints with associated generalized coordinates $\boldsymbol{q} \in \mathbb{R}^n$. A spatial motion task for the robot is specified in terms of task coordinate variables $\boldsymbol{x} \in \mathbb{R}^m$, with $m \leq n$ (e.g., the end-effector pose, or the position of a point along the robot structure). These coordinates are related by the direct and differential kinematic equations

$$\boldsymbol{x} = \boldsymbol{f}(\boldsymbol{q}), \qquad \dot{\boldsymbol{x}} = \boldsymbol{J}(\boldsymbol{q})\dot{\boldsymbol{q}}, \qquad (1)$$

where $\boldsymbol{J}(\boldsymbol{q}) = \partial \boldsymbol{f}(\boldsymbol{q})/\partial \boldsymbol{q}$ is the so-called task Jacobian matrix (obtained by analytic differentiation).

The dynamic model of the robot is

$$\boldsymbol{M}(\boldsymbol{q})\ddot{\boldsymbol{q}} + \boldsymbol{C}(\boldsymbol{q}, \dot{\boldsymbol{q}})\dot{\boldsymbol{q}} + \boldsymbol{g}(\boldsymbol{q}) = \boldsymbol{\tau} + \boldsymbol{\tau}_{ext}, \qquad (2)$$

where $\boldsymbol{M}(\boldsymbol{q})$ is the symmetric, positive definite inertia matrix, the Coriolis and centrifugal terms are factorized using the matrix $\boldsymbol{C}(\boldsymbol{q}, \dot{\boldsymbol{q}})$ of Christoffel symbols, $\boldsymbol{g}(\boldsymbol{q})$ is the gravity vector, $\boldsymbol{\tau}$ is the control torque performing work on $\boldsymbol{q}$, and $\boldsymbol{\tau}_{ext}$ is the torque due to external/environmental generalized forces acting on the robot.

If $\boldsymbol{F}_k \in \mathbb{R}^{m_k}$ is an external force applied to a generic point of the robot and $\boldsymbol{J}_k(\boldsymbol{q})$ is the $m_k \times n$ (geometric) Jacobian matrix associated to the contact point on the robot, the external torque in (2) will have the expression

$$\boldsymbol{\tau}_{ext} = \boldsymbol{J}_k^T(\boldsymbol{q})\boldsymbol{F}_k. \qquad (3)$$

Note that in general neither the external force $\boldsymbol{F}_k$ nor the location of a possible collision (and thus the associated $\boldsymbol{J}_k^T(\boldsymbol{q})$) are known, in the absence of external/tactile sensing.

For the sake of simplicity, in the following we will consider only rigid robots with rigid transmissions/joints. However, all the methods presented in this paper can be extended also to robots with elastic joints and to VSA-based robots.

III. COLLISION DETECTION

Detection of physical collisions is the basic innermost feature for a safe control of the robot behavior, since collision avoidance cannot be always guaranteed in unpredictable dynamic environments. To be useful, collision detection must be very efficient, in order to allow a fast robot reaction. This limits the use of exteroceptive sensors, such as cameras, due to their low bandwidth. Moreover, achieving detection based only on basic proprioceptive sensors is very appealing in terms of on-board availability (without workspace restrictions) and limited costs.

In this work, we use the residual-based method originally proposed in [5] for estimating the effect of external forces arising in a collision during robot motion. This method needs an accurate knowledge of the dynamic model terms in (2), but uses only robot joint position measurements, as given, e.g., by encoders. The further availability of torque sensing at the robot joints can be easily incorporated (in case of elastic transmissions [6] or VSA joints [12]), but is not strictly needed.

Based on the generalized momentum of the robot

$$\boldsymbol{p} = \boldsymbol{M}(\boldsymbol{q})\dot{\boldsymbol{q}}, \qquad (4)$$

we define a residual signal $\boldsymbol{r} \in \mathbb{R}^n$ as follows:

$$\boldsymbol{r}(t) = \boldsymbol{K}_I \left(\boldsymbol{p}(t) - \int_0^t \left(\boldsymbol{\tau} + \boldsymbol{C}^T(\boldsymbol{q}, \dot{\boldsymbol{q}})\dot{\boldsymbol{q}} - \boldsymbol{g}(\boldsymbol{q}) + \boldsymbol{r} \right) ds \right), \qquad (5)$$

with $\boldsymbol{r}(0) = \boldsymbol{0}$ and a diagonal gain matrix $\boldsymbol{K}_I > 0$ (we also assume that the robot is initially at rest, $\boldsymbol{p}(0) = \boldsymbol{0}$). Note that the source of the control input torque $\boldsymbol{\tau}$ in (5) is irrelevant, i.e., it can be either an open-loop command or any computed feedback law. From (2) and (4), the dynamics of $\boldsymbol{r}$ is

$$\dot{\boldsymbol{r}} = \boldsymbol{K}_I \left(\boldsymbol{\tau}_{ext} - \boldsymbol{r} \right), \qquad (6)$$

i.e., each component r_i is an independent, first-order, unity-gain filtered version of the unknown $\tau_{ext,i}$, with the gain $K_{I,i}$ as filter bandwidth. In the ideal condition $\boldsymbol{K}_I \to \infty$, which means in practice that the gains should be taken as large as possible, we have

$$\boldsymbol{r} \simeq \boldsymbol{\tau}_{ext}. \qquad (7)$$

A physical collision will then be detected as soon as, e.g., $\|\boldsymbol{r}\| > r_{thres}$, being $r_{thres} > 0$ a suitable scalar threshold used to prevent false detection due to measurement noise and/or model uncertainties on $\boldsymbol{r}$. Note also that when the contact/collision is definitely over, the residual $\boldsymbol{r}$ will return to zero according to (6).

A useful interpretation of this collision detection method is that, thanks to the residual computation, we are able to compensate for the coupled accelerations and dynamic motion of the robot and treat the problem as if it was a quasi-static one. In fact, using (3) and (6), only the components of the residual vector that are associated to joints placed *before* (in the robot chain) the single colliding link will be influenced by the collision force $\boldsymbol{F}_k$ (the last few rows of $\boldsymbol{J}_k^T(\boldsymbol{q})$ are zero in this case). This basic property, in association with an external system able to locate accurately the collision point, will be used later for estimating the actual contact force $\boldsymbol{F}_k$.

The residual generation is a flexible tool. For instance, consider a situation in which an *intentional* physical interaction should occur between a human operator and the robot end-effector, equipped with a wrist F/T sensor. We can still detect *undesired* collisions by a slight modification of (5). In this case, the right-hand side of the robot dynamics (2 should be modified as $\boldsymbol{\tau} + \boldsymbol{J}_e^T(\boldsymbol{q})\boldsymbol{F}_m + \boldsymbol{\tau}_{ext}$, being $\boldsymbol{F}_m$ the force/torque measured by the wrist sensor, $\boldsymbol{J}_e(\boldsymbol{q})$ the geometric Jacobian associated to the robot end-effector (i.e., where the F/T sensor is mounted). As a result, the joint torque $\boldsymbol{\tau}_{ext}$ due to an undesired collision is detectable by the modified residual

$$
\begin{aligned}
\boldsymbol{r}(t) = \boldsymbol{K}_I \Big(\boldsymbol{p}(t) - \int_0^t \big(\boldsymbol{\tau} + \boldsymbol{J}_e^T(\boldsymbol{q})\boldsymbol{F}_m \\
+ \boldsymbol{C}^T(\boldsymbol{q},\dot{\boldsymbol{q}})\dot{\boldsymbol{q}} - \boldsymbol{g}(\boldsymbol{q}) + \boldsymbol{r} \big) ds \Big),
\end{aligned} \tag{8}
$$

which will behave again as (6).

IV. COLLISION REACTION

With reference to the general scheme of Fig. 1, once an undesired physical collision has been detected the robot switches as fast as possible from the control law associated to normal task execution to a reaction control law. A series of alternative reaction strategies have been considered and implemented, see, e.g., [6], [7], [19]. Not all of them abandon completely the original task execution. For instance, a time scaling of the original joint or Cartesian trajectory can be realized [7], so that the robot stops or moves back along the past path and recovers forward motion along the planned path only once the collision is over. In [19], the redundancy of the robot with respect to the original task (e.g., the end-effector tracking a desired trajectory) is exploited by accommodating the robot reaction command in a suitable dynamic null space so as to preserve task execution in full or partially, provided that the residual signal $\boldsymbol{r}$ does not reach a higher safety threshold: otherwise, the persistent contact may lead to a potential human injury, and then the task is eventually abandoned. A portfolio of available reaction strategies is shown in Fig. 2.

In the present framework, we consider two further direct uses of the residual $\boldsymbol{r}$ which produce a controlled motion that safely pushes the robot away from the collision area.

The first reaction law is a modified version of the *reflex* strategy introduced in [6] and is based again on the full knowledge of the robot dynamics. With reference to (2),
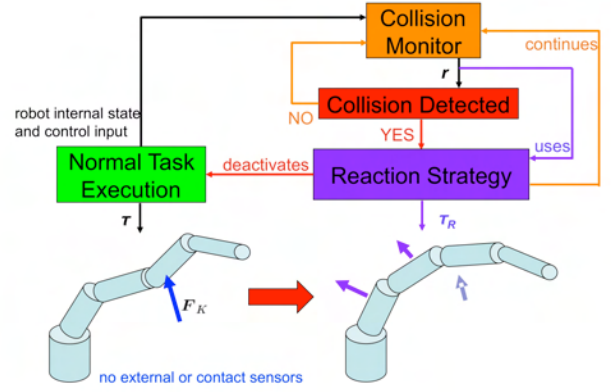

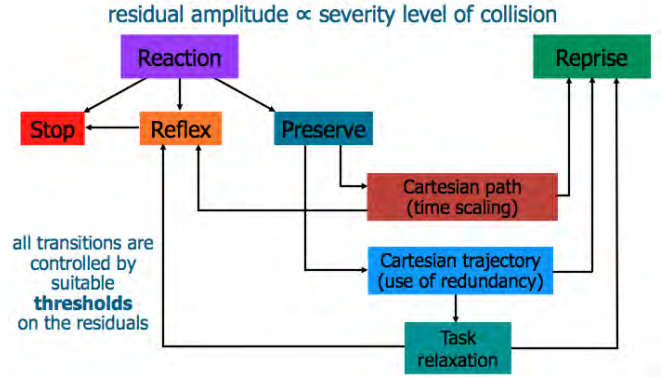Fig. 1.   Collision detection and reaction conceptual scheme

Fig. 2.   Portfolio of developed reaction strategies

where now the presence of an external torque $\boldsymbol{\tau}_{ext}$ has been detected, define the reaction control law as

$$
\boldsymbol{\tau} = \boldsymbol{M}(\boldsymbol{q})\left(\boldsymbol{K}_R \boldsymbol{r} - \boldsymbol{D}_R \dot{\boldsymbol{q}} \right) + \boldsymbol{C}(\boldsymbol{q},\dot{\boldsymbol{q}})\dot{\boldsymbol{q}} + \boldsymbol{g}(\boldsymbol{q}) - \boldsymbol{r}, \tag{9}
$$

with reaction gain $\boldsymbol{K}_R = k_R \boldsymbol{I} > 0$ and velocity damping $\boldsymbol{D}_R = d_R \boldsymbol{I} > 0$. Assuming the validity of (7), by virtue of the cancelations induced by this type of feedback linearization law, the closed-loop system (2–9) becomes approximately

$$
\ddot{\boldsymbol{q}} = \boldsymbol{K}_R \boldsymbol{r} - \boldsymbol{D}_R \dot{\boldsymbol{q}}. \tag{10}
$$

As a consequence, the robot acceleration at the collision point will be

$$
\begin{aligned}
\ddot{\boldsymbol{x}}_k &= \boldsymbol{J}_k(\boldsymbol{q})\ddot{\boldsymbol{q}} + \dot{\boldsymbol{J}}(\boldsymbol{q})\dot{\boldsymbol{q}} = k_R \boldsymbol{J}_k(\boldsymbol{q})\boldsymbol{r} + \left(\dot{\boldsymbol{J}}(\boldsymbol{q}) - \boldsymbol{D}_R \right)\dot{\boldsymbol{q}} \\
&\simeq k_R \boldsymbol{J}_k(\boldsymbol{q})\boldsymbol{J}_k^T(\boldsymbol{q})\boldsymbol{F}_k,
\end{aligned} \tag{11}
$$

where the velocity dependent terms have been neglected, thanks to the presence of velocity damping in the reaction. The final outcome is that the instantaneous robot acceleration at the collision/contact area will be along (although not exactly aligned with) the direction of the collision force, since

$$
\boldsymbol{F}_k^T \ddot{\boldsymbol{x}}_k = k_R \boldsymbol{F}_k^T \boldsymbol{J}_k(\boldsymbol{q})\boldsymbol{J}_k^T(\boldsymbol{q})\boldsymbol{F}_k = k_R \boldsymbol{\tau}_{ext}^T \boldsymbol{\tau}_{ext} \geq 0. \tag{12}
$$

The second reaction law is simpler to implement in the presence of low-level high-gain/high-rate control loops at

the robot joints that are approximately able to impose a commanded reference velocity $\dot{q}_r$. In this case, a reaction strategy based on the so-called *admittance control* is realized by choosing

$$\dot{q}_r = K_Q r, \tag{13}$$

with reaction gain $K_Q = k_Q I > 0$. The name follows from the fact that a robot velocity is generated in reaction to the detected collision torque. Assuming $\dot{q} \simeq \dot{q}_r$, the robot velocity at the collision point will be

$$\dot{x}_k = J_k(q)\dot{q} \simeq k_Q J_k(q) J_k^T(q) F_k, \tag{14}$$

so that a relation similar to (12) is found for $F_k^T \dot{x}_k \geq 0$. As it will be shown in Sect. V, a convenient feature of the admittance control scheme is that its structure remains the same both when the robot needs to react to a dynamic torque due to a *physical* collision and when a robot reaction is induced by an *artificial* repulsive potential designed for collision avoidance.

V. COLLISION AVOIDANCE

Avoiding an undesired collision is indeed the safest approach for human-robot coexistence. The main information needed by any on-line collision avoidance algorithm is the relative distance between the robot and some obstacle in its workspace, as acquired by exteroceptive sensors either fixed in the environment or mounted on the robot. The performance of the algorithm depends also on the fast processing capability of the sensor data. In [4], we have proposed a new efficient method for estimating obstacle-to-robot distances that wokrs directly in the depth space associated to a depth sensor (e.g., a Kinect monitoring the HRI scene).

Consider a generic point of interest P that belongs to the robot body. For every depth image pixel O in a suitable region of surveillance S we generate a repulsive action

$$V_C(P, O) = v(P, O)\frac{D(P, O)}{\|D(P, O)\|}, \tag{15}$$

where $D(P, O)$ is the vector between the point of interest and the obstacle point associated to O, computed with the method presented in [4], while the magnitude of V_C is designed as

$$v(P, O) = \frac{V_{max}}{1 + e^{\|D(P, O)\|(2/\rho)\alpha - \alpha}}, \tag{16}$$

being V_{max} a maximum admissible magnitude, $\rho > 0$ the side length of the surveillance area, and $\alpha > 0$ a factor shaping the repulsive profile. To generate the repulsive vector associated to P in a robust way, we use all obstacle points that lie inside the region of surveillance:

$$V_{C_T}(P, O) = \sum_{O \in S} V_C(P, O),$$
$$V_{C_{all}}(P) = v(P, O_{min})\frac{V_{C_T}(P, O)}{\|V_{C_T}(P, O)\|}. \tag{17}$$

While all obstacle points contribute to the direction of the resulting repulsive vector, its magnitude depends only on the obstacle point with minimum distance

$$O_{min} = \text{argmin}_{O \in S}\|D(P, O)\|. \tag{18}$$

A typical example of repulsive vector computation is shown in Fig. 3.
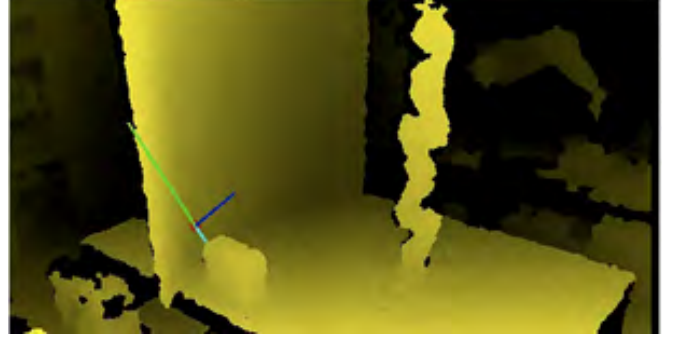

Fig. 3. Example of repulsive vector computation. Lighter colors refer to obstacle points with smaller depth, the point of interest P is represented by a red circle, and the minimum distance is represented in cyan. The repulsive vector obtained by using only the obstacle point of minimum distance (in green) provides a misleading information, while the one obtained by using all points in the range of surveillance (in blue) points to a free (safer) area

The repulsive vector in (17–18) can be used as input of a generic collision avoidance algorithm, i.e., based on potential fields [20], circular fields [21], or elastic strips [22]. Indeed, multiple points of interest are distributed along the robot manipulator, including its end-effector. However, we use two different collision avoidance schemes for the end-effector and for all other points of the robot, as proposed in [4]. The repulsive vector associated to the end-effector P_e is directly considered as repulsive velocity that modifies its original desired task velocity $\dot{x}_t$ simply as

$$\dot{x}_r = \dot{x}_t + V_{C_{all}}(P_e). \tag{19}$$

This is translated into a desired joint velocity, e.g., through Jacobian pseudoinversion $\dot{q}_r = J_e^{\#}(q)\dot{x}_r$. On the other hand, the repulsive vectors associated to each of the other points of interest P_r on the robot are considered as artificial forces that will modify the feasible robot motion when mapped in the joint space as

$$S_{P_r} = J_{P_r}^T(q)V_{C_{all}}(P_r), \tag{20}$$

where $J_{P_r}(q)$ is the Jacobian associated to the robot point P_r. As proposed in [23], a convenient way for using the artificial terms S_{P_r} is to modify accordingly the instantaneous joint velocity bounds: joint motions that will move the robot point P_r toward an obstacle will be slowed down by shrinking on the proper side the available range of joint velocity components.

VI. SAFE COLLABORATION

In a safe coexistence phase, the human operator and the robot share the same workspace without necessarily undergoing physical interaction. A collaboration phase can be requested either by the human or by the robot, through some form of contactless interaction. According to the goals of each collaborative task, one can identify which (collaborative) parts or points of the robot and, similarly, which parts of the human should be involved in the specific physical

interaction. During safe physical collaboration, only contacts between the prescribed human and robot collaborative parts are allowed, while all other contacts are considered as unintended collisions and must be avoided.

A. Contactless interaction

A contactless interaction is the simplest form of collaboration, typically involving an exchange of information or commands implicitly associated to the shared task. In the present case, the contactless interaction phase allows the human operator to make a request of collaboration to the robot through the following steps:

- recognize the collaboration request;
- if it is not implicit in the request, recognize the human/robot collaborative parts;
- complete the current task in operation or abort it (if possible), and communicate to the counterpart to wait if needed;
- start the physical collaboration phase.

Note that the same human-to-robot steps are valid also for robot-to-human communication.
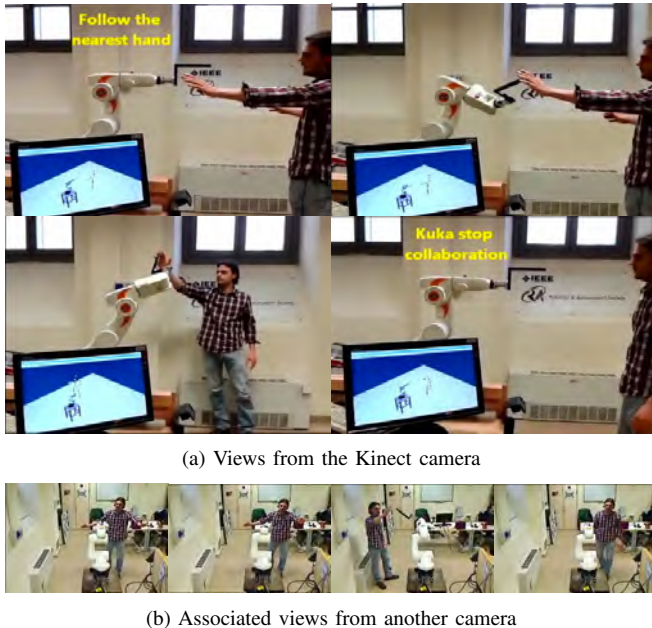

(a) Views from the Kinect camera

(b) Associated views from another camera

Fig. 4. Contactless interaction: Image flow after issuing a 'follow the nearest hand' vocal command, until interaction is stopped by another vocal command

The collaboration request can be communicated using gestures, vocal commands, or a combination of the two. When the human request is done with a gesture (e.g., hand waving in the presented experiments), his/her collaborative part is the one used for the gesture. If voice were used, the collaborative part can be expressed in the vocal command (e.g., 'follow the right hand') or combined with the gesture (e.g., 'follow the hand', showing the right hand). Figure 4 shows an example of contactless interaction using a KUKA KR5 sixx R650 robot, a Kinect depth/camera sensor, and a standard voice recognition software (Microsoft SAPI 5.1).

B. Contact force estimation

Physical collaboration is characterized by force exchanges between human and robot, which may occur at any place of the robot structure (as in whole arm manipulation). In the absence of a distributed force/tactile measurement system, an indirect evaluation of the contact force is needed. We propose here to combine our residual-based method for collision detection of Sect. III with the external information gathered for collision avoidance of Sect. V.

Suppose that a single contact occurs with a generalized force $\boldsymbol{F}_k$ applied by the human to the robot (no matter if in motion or standing still). The residual $\boldsymbol{r}$ contains an indirect estimate of $\boldsymbol{F}_k$, being from eqs. (3) and (7)

$$\boldsymbol{r} \simeq \boldsymbol{\tau}_{ext} = \boldsymbol{J}_k^T(\boldsymbol{q})\boldsymbol{F}_k. \tag{21}$$

If the anticipated contact point, as extracted from the minimum distance data obtained by the external (depth) sensor, belongs to the allowed collaborative parts of the robot and the human, both the collision avoidance and the robot reaction based on the residual will be disabled. At this stage, the depth sensor information can be used to localize the contact point and, from the measure of the current robot joint position, we are also able to compute the associated Jacobian $\boldsymbol{J}_k(\boldsymbol{q})$. Therefore, the external force can be approximately estimated by pseudoinversion as

$$\widehat{\boldsymbol{F}}_k = (\boldsymbol{J}_k^T(\boldsymbol{q}))^{\#}\boldsymbol{r}. \tag{22}$$

Note that the estimate will be limited to only those components of $\boldsymbol{F}_k$ that can be detected by the residual $\boldsymbol{r}$. From (21), all forces $\boldsymbol{F}_k \in \mathcal{N}(\boldsymbol{J}_k^T(\boldsymbol{q}))$ will not be recovered in $\widehat{\boldsymbol{F}}_k$. However, this should not be considered as a serious limitation since such force components do not produce active work on the robot coordinates $\boldsymbol{q}$, as discussed also in [6].

Equation (22) can be extended to the case of multiple simultaneous contact points. For simplicity, consider just two contact forces ($k = 1, 2$). We have then

$$\begin{pmatrix} \widehat{\boldsymbol{F}}_1 \\ \widehat{\boldsymbol{F}}_2 \end{pmatrix} = \begin{pmatrix} \boldsymbol{J}_1^T(\boldsymbol{q}) & \boldsymbol{J}_2^T(\boldsymbol{q}) \end{pmatrix}^{\#}\boldsymbol{r}. \tag{23}$$

As before, the estimation will be intrinsically limited to the components of each contact force not lying in the kernel of the respective Jacobian transpose.

C. Collaboration and safety

As already mentioned in our control hierarchy, when the robot is physically collaborating with a human the need of a safe coexistence must continue to be preserved. This implies that the presented collision avoidance, detection, and reaction schemes should be used also during a collaboration phase, in order to avoid any undesired contact, i.e., a collision between robot and human parts that are not intended to be collaborative. In particular, such behavior is translated into allowing a desired contact while the collision avoidance algorithm is active. To do this, we simply remove from the depth image all points in a suitable region close to the collaborative parts, as illustrated in Fig. 5. Removed points

do not generate a repulsive action, allowing the collaborative human part to touch the robot.

Fig. 5. Snapshot of a collaboration experiment. In the box on the right, the associated depth image shows, highlighted by a blue circle, the collaborative human part (the right hand) that has been removed

A different approach has to be used for collision detection module. When the human is physically collaborating with the robot, it is too difficult to separate collaboration forces from collision forces in the residual. Physical collision detection is then turned off, leaving to the collision avoidance module the task to prevent accidental contacts.

VII. Experimental results

The integrated pHRI control approach has been tested on a scenario in which a robot manipulator is executing a motion task through a sequence of desired Cartesian points and a human operator enters in its workspace (safe coexistence). When the human operator requests a collaboration phase using gestures, the robot recognizes the gesture and starts the collaboration. During this phase the human can exchange forces with the robot end-effector, using the hand that has activated the collaboration. All other human parts, as well as all other possible obstacles, are avoided (safe physical collaboration). The collaboration phase terminates when the human pushes on the robot wrist. The experiments are shown in the accompanying video clip.

A. Set-up

Experiments have been performed with a KUKA LWR-IV, a 7R torque-controlled manipulator with a control cycle of 1 ms. The workspace is monitored by a Microsoft Kinect depth sensor, positioned at a radial distance of 2 m and at a height of 1.2 m w.r.t. the robot base frame. The Kinect captures a 640×480 depth image with a frequency of 30 Hz. The proposed collision avoidance and physical collaboration algorithms are executed on an eight-core CPU: four processors are used for the repulsive velocity computations, and the other four enable visualization and robot motion control.

B. Safe coexistence

In the first part of the experiment, the robot and the human operator perform two independent tasks in the same workspace. The robot task consists in cyclic moving its end-effector through three Cartesian positions ($n = 7$, $m = 3$, with degree of redundancy $n - m = 4$). As shown in Fig. 6, when the human crosses the end-effector trajectory, our algorithm allows the robot to continue the task while avoiding collisions. Figure 7 shows the robot end-effector

trajectory in the absence of the human obstacle and in the case of collision avoidance needed.
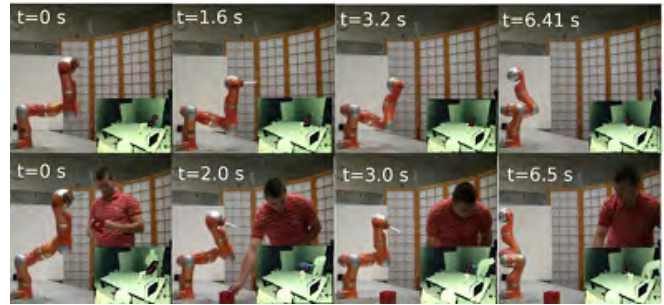

Fig. 6. Safe coexistence: Image flow for a motion through three points in the absence of dynamic obstacles (top) and simultaneous collision avoidance of a human entering the workspace (bottom)
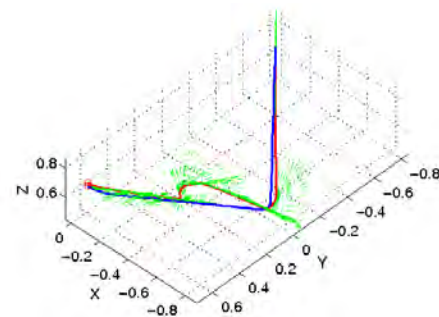

Fig. 7. Safe coexistence: Robot end-effector trajectories in the absence of dynamic obstacles (blue line) and in the case of collision avoidance of a human entering the workspace (red line). The green segments represent the commanded Cartesian velocities

C. Physical collaboration

While the robot is performing its task, the human requests the start of a collaboration using a predefined gesture (hand waving). In the collaboration phase, the robot follows the human hand that has activated the collaboration. Physical contact is established between the collaborating hand and the robot. A plot of the positional coordinates X, Y, and Z of the robot end-effector and of the collaborating hand during different phases of the collaboration is reported in Fig. 8. Figure 9 shows the image flow of an example of collaborating phase.
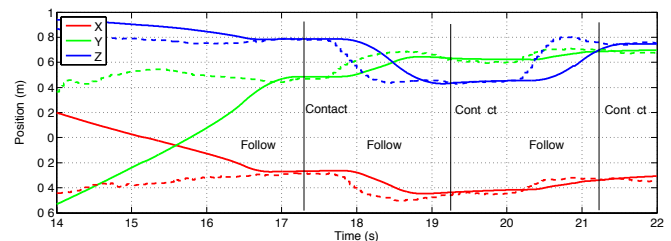

Fig. 8. Physical collaboration: Trajectories of the positional components of the robot end-effector (solid) and the collaborative hand (dashed)
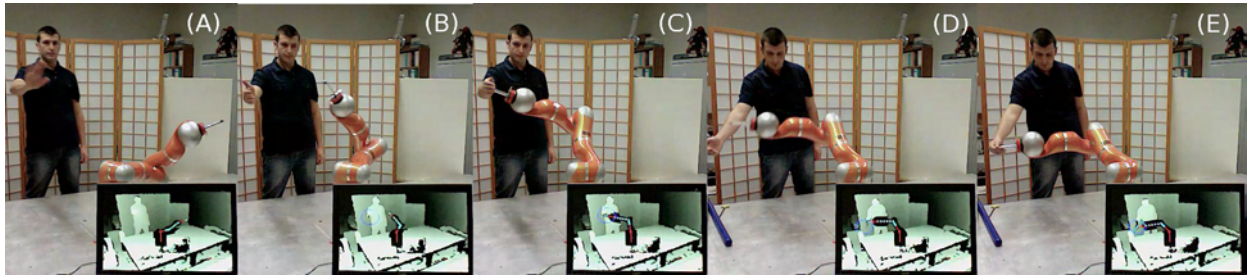
Fig. 9. Physical collaboration: The human activates collaboration using a predefined gesture (A); the robot tracks the collaborating right hand (B), reaching physical contact (C); the human moves away the right hand (D) and the robot follows it until reaching a new contact (E)
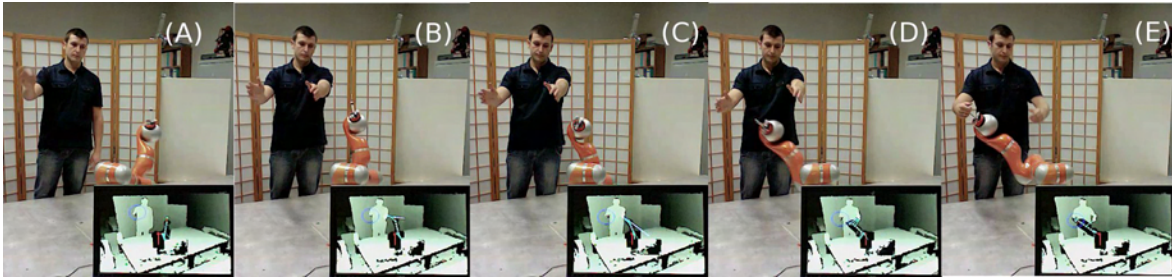

Fig. 10. Safe pHR collaboration: The human activates collaboration using a predefined gesture (A); the robot moves toward the collaborative hand while an unforeseen obstacle (the other hand) crosses the robot trajectory (B); collision is avoided (C-D) and the collaborative hand is reached (E)
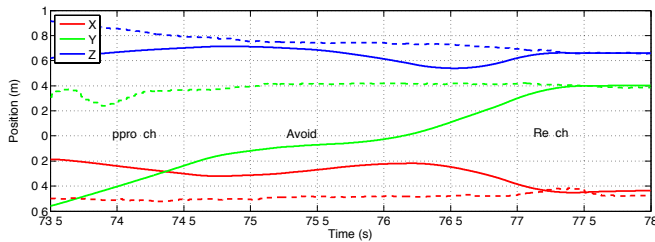

Fig. 11. Safe pHR collaboration: Trajectories of the positional components of the robot end-effector (solid) and the collaborative hand (dashed) for Fig. 10

D. Safe pHR collaboration

Human safety must be guaranteed also during the physical collaborative phase, and the robot has to avoid any collision with human parts different from the hand that engaged the collaboration. Figure 10 shows a case where the human places his left hand across the robot trajectory during a collaboration with the right hand. Collision is avoided with the left hand while the robot still reaches the collaborative right hand. The plot of the positional coordinates X, Y, and Z of the robot end-effector and of the collaborating hand during the experiment is reported in Fig. 11. Consistently with the safe coexistence requirement, all other obstacles as well as non-collaborative parts of the human are avoided by the robot. This behavior is also shown in Fig. 12, where the human puts his leg across the trajectory of the robot elbow, while the robot end-effector reaches the collaborative hand avoiding any other collision.

VIII. Conclusions

We have presented a unified framework for safe physical human-robot interaction, based on a hierarchy of consistent behaviors that the robot must accomplish. A collision avoidance algorithm based on depth images is used to obtain safe human-robot coexistence. Since collisions cannot be always avoided in principle, a collision detection and reaction algorithm based on a residual signal generated using only joint position measurements is integrated in the same strategy. The same residual can be used to perform a number of different reflex reactions that push the robot away from the collision area.

The second part of our control framework covers physical human-robot collaboration tasks, which are activated or ended by the human using predefined gestures or voice commands. During a collaboration phase, contact forces between the robot and the human occurring at any relative location can be estimated by using together the residual and the knowledge of the contact point obtained from depth sensing. Moreover, only the designated robot and human collaborating parts are allowed to physically interact, while the robot continues to avoid any other part of the human body, as well as other static or dynamic obstacles. Preliminary experiments using a KUKA LWR-IV robot and a Kinect sensor have shown the good overall performance of the proposed approach.

In our future work within the SAPHARI project, we are going to explore further collaboration modalities, in which the robot behavior takes also into account where the human is focused or predicting an incipient collaboration phase by interpreting the human motion. Moreover, alternative collision avoidance algorithms will be tested in our Lab and
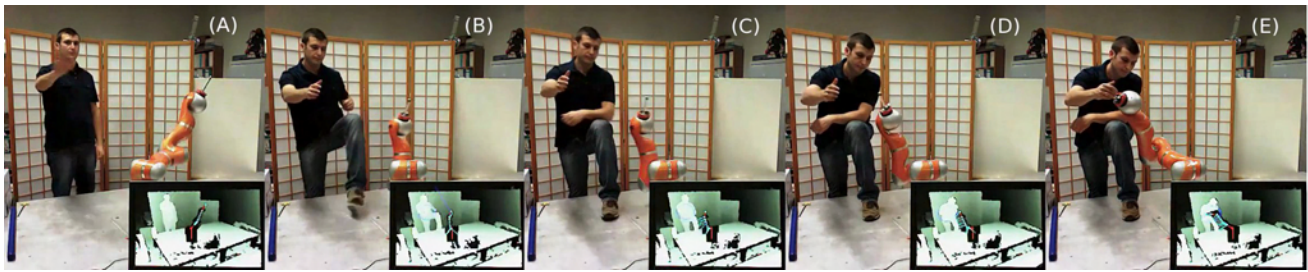
Fig. 12. Safe pHR collaboration: The human activates collaboration using a predefined gesture (A); the robot moves toward the collaborative hand while an unforeseen obstacle (the human's leg) crosses the robot trajectory (B); the collaborative hand is reached avoiding the space occupied by all non-collaborative parts (C-E)

the collision detection/reaction method will be extended so as to work in parallel to the physical collaboration phase. Another important step will be to design, implement, and validate generalized force/impedance control schemes based on the contact forces estimated through the combined use of residuals, proprioceptive and exteroceptive sensors.

REFERENCES

[1] ISO 10218-1-2011. Robots and robotic devices – Safety requirements for industrial robots. Part 1: Robots; Part 2: Robot systems and integration. [Online]. Available: http://www.iso.org (since July 1, 2011).

[2] S. Haddadin, "Towards Safe Robots: Approaching Asimovs 1st Law," Ph.D. dissertation, Rheinisch-Westfälischen Technischen Hochschule, Aachen, Germany, Oct. 2011.

[3] R. Schiavi, F. Flacco, and A. Bicchi, "Integration of active and passive compliance control for safe human-robot coexistence," in *Proc. 2009 IEEE Int. Conf. on Robotics and Automation*, 2009, pp. 259–264.

[4] F. Flacco, T. Kröger, A. De Luca, and O. Khatib, "A depth space approach to human-robot collision avoidance," in *Proc. IEEE Int. Conf. on Robotics and Automation*, St. Paul, MN, May 2012.

[5] A. De Luca and R. Mattone, "Sensorless robot collision detection and hybrid force/motion control," in *Proc. IEEE Int. Conf. on Robotics and Automation*, 2005, pp. 1011–1016.

[6] A. De Luca, A. Albu-Schäffer, S. Haddadin, and G. Hirzinger, "Collision detection and safe reaction with the DLR-III lightweight robot arm," in *Proc. IEEE/RSJ Int. Conf. on Intelligent Robots and Systems*, 2006, pp. 1623–1630.

[7] S. Haddadin, A. Albu-Schaffer, A. De Luca, and G. Hirzinger, "Collision detection and reaction: A contribution to safe physical human-robot interaction," in *Proc. IEEE/RSJ Int. Conf. on Intelligent Robots and Systems*, Nice, F, September 2008, pp. 3356–3363.

[8] R. Schiavi, G. Grioli, S. Sen, and A. Bicchi, "VSA-II: A novel prototype of variable stiffness actuator for safe and performing robots interacting with humans," in *Proc. IEEE Int. Conf. on Robotics and Automation*, 2008, pp. 2171–2176.

[9] A. Jafari, N. Tsagarakis, B. Vanderborght, and D. Caldwell, "An intrinsically safe actuator with the ability to adjust the stiffness," in *7th IARP Work. on Technical Challenges for Dependable Robots in Human Environments*, 2010.

[10] O. Eiberger, S. Haddadin, M. Weis, A. Albu-Schäffer, and G. Hirzinger, "On joint design with intrinsic variable compliance: Derivation of the DLR QA-joint," in *Proc. IEEE Int. Conf. on Robotics and Automation*, 2010, pp. 1687–1694.

[11] A. Bicchi and G. Tonietti, "Fast and soft arm tactics: Dealing with the safety-performance trade-off in robot arms design and control," *IEEE Robotics and Automation Mag.*, vol. 11, no. 2, pp. 22–33, 2004.

[12] A. De Luca, F. Flacco, A. Bicchi, and R. Schiavi, "Nonlinear decoupled motion-stiffness control and collision detection/reaction for the VSA-II variable stiffness device," in *Proc. IEEE/RSJ Int. Conf. on Intelligent Robots and Systems*, 2009, pp. 5487–5494.

[13] G. Hirzinger, A. Albu-Schäffer, M. Hähnle, I. Schaefer, and N. Sporer, "On a new generation of torque controlled light-weight robots," in *Proc. IEEE Int. Conf. on Robotics and Automation*, 2001, pp. 3356–3363.

[14] O. Khatib, K. Yokoi, O. Brock, K.-S. Chang, and A. Casal, "Robots in human environments: Basic autonomous capabilities," *Int. J. of Robotics Research*, vol. 18, no. 7, pp. 684–.696, 1999.

[15] N. Mansard, O. Khatib, and A. Kheddar, "A unified approach to integrate unilateral constraints in the stack of tasks," *IEEE Trans. on Robotics*, vol. 25, no. 3, pp. 670–685, 2009.

[16] O. Rogalla, M. Ehrenmann, R. Zollner, R. Becher, and R. Dillmann, "Using gesture and speech control for commanding a robot assistant," in *Proc. IEEE Int. Workshop on Robot and Human Interactive Communication*, 2002, pp. 454–459.

[17] C. Nehaniv, K. Dautenhahn, J. Kubacki, M. Haegele, C. Parlitz, and R. Alami, "A methodological approach relating the classification of gesture to identification of human intent in the context of human-robot interaction," in *Proc. IEEE Int. Workshop on Robot and Human Interactive Communication*, 2005, pp. 371–377.

[18] J. Mainprice, E. Sisbot, T. Simeon, and R. Alami, "Planning safe and legible hand-over motions for human-robot interaction," in *Proc. IARP Workshop on Tech. Challenges for Dependable Robots in Human Environments*, 2010.

[19] A. De Luca and L. Ferrajoli, "Exploiting robot redundancy in collision detection and reaction," in *Proc. IEEE/RSJ Int. Conf. on Intelligent Robots and Systems*, 2008, pp. 3299–3305.

[20] O. Khatib, "Real-time obstacle avoidance for manipulators and mobile robots," *Int. J. of Robotics Research*, vol. 5, no. 1, pp. 90–98, 1986.

[21] S. Haddadin, S. Belder, and A. Albu-Schaeffer, "Dynamic motion planning for robots in partially unknown environments," in *IFAC World Congress (IFAC2011)*, Milan, Italy, September 2011.

[22] O. Brock and O. Khatib, "Elastic strips: A framework for motion generation in human environments." *Int. J. of Robotics Research*, vol. 21, no. 12, pp. 1031–1052, 2002.

[23] F. Flacco, A. De Luca, and O. Khatib, "Motion control of redundant robots under joint constraints: Saturation in the null space," in *Proc. IEEE Int. Conf. on Robotics and Automation*, St. Paul, MN, USA, May 2012.